Organic & Biomolecular Chemistry

Impacts of Noncovalent Interactions Involving Sulfur Atoms on Protein Stability, Structure, Folding, and Bioactivity

Journal:	*Organic & Biomolecular Chemistry*
Manuscript ID	OB-REV-09-2022-001602.R1
Article Type:	Review Article
Date Submitted by the Author:	24-Oct-2022
Complete List of Authors:	Kojasoy, Volga; Bogazici Universitesi, Tantillo, Dean; University of California, Davis, Chemistry;

ARTICLE

Impacts of Noncovalent Interactions Involving Sulfur Atoms on Protein Stability, Structure, Folding, and Bioactivity

Received 00th January 20xx,
Accepted 00th January 20xx

DOI: 10.1039/x0xx00000x

Volga Kojasoy and Dean J. Tantillo*

This review discusses the various types of noncovalent interactions in which sulfur atoms participate and their effects on protein stability, structure, folding and bioactivity. Current approaches and recommendations for modelling these noncovalent interactions (in terms of both geometries and interaction energies) are highlighted.

Volga Kojasoy was raised in Istanbul, Turkey. She obtained a B.S. in Chemistry from Bogazici University and then moved to UC Davis in 2018, where she is now a Ph.D. student under the guidance of Prof. Dean Tantillo. Her current research interests include natural products biosynthesis and noncovalent interactions.

Dean Tantillo was born and raised in Quincy, Massachusetts, USA. He received an A.B. degree in Chemistry in 1995 from Harvard and a Ph.D. in 2000 from UCLA (with Ken Houk) and then moved to Cornell where he did postdoctoral research with Roald Hoffmann. Dean joined the faculty at UC Davis in 2003. Research in Dean's group is driven by puzzling mechanistic questions in the areas of biosynthesis, organometallic chemistry, and stereoselective synthetic reactions, with a focus on cyclization/rearrangement reactions used by Nature and by chemists to synthesize complex natural products. He is particularly interested these days in non-statistical dynamic effects, entropy and organic photochemistry.

1. Introduction

How does the presence of sulfur atoms in proteins affect structure, stability, and bioactivity? The conformational stability of a protein is characterized as the free energy change between its folded and unfolded states, which generally amounts to 5-15 kcal mol^{-1}.[1–5] A balance (sometimes compromise) between many individual (but often interdependent) noncovalent interactions generates each unique folded structure.[2,4,6,7] Noncovalent interactions involving sulfur atoms (S), although generally receiving less attention than those involving oxygen and nitrogen, play essential roles in protein structure and, as a result, stability, and function.[8–11]

Many examples of interactions involving sulfur have been shown to have important biological consequences. For example, the attractive electrostatic interaction between sulfur and oxygen atoms in thiazole nucleoside analogues was found to be important for their antitumor activity.[12] Sulfur, being a highly polarizable atom, is able to participate in strong dispersion interactions that allow the sulfur containing amino acids methionine (Met) and cysteine (Cys) to make large contributions to the overall 3-dimensional structure and function of membrane proteins.[13] While the formation of disulfide bonds between Cys residues is a key means of stabilizing the tertiary structure of a protein, Brandt et al. revealed that the cleavage of disulfide bonds promoted by sulfur-oxygen interactions can play a critical role in receptor activation.[14] It also was shown that the reduction of disulfide bonds to thiols—a reaction that modifies that types of noncovalent interactions available for the Cys residues involved—impairs the binding affinity of SARS-CoV/CoV-2 spike protein to the angiotensin-converting enzyme 2, which is the receptor that enables entering the host cells.[15]

There have been many excellent reviews on the importance of noncovalent interactions in biological systems, for example, those by Diederich,[10,16,17] Meanwell,[18] Stahl,[19] Schreiner,[9] and Raines.[11] Of particular note is Meanwell and co-workers' review on applications of noncovalent interactions involving sulfur in drug design. Here we provide a catalog of types of noncovalent interactions involving sulfur atoms, along with details of from computational studies on their physical nature and examples of

Department of Chemistry, University of California, Davis, 1 Shields Avenue, Davis, CA, 95616, USA.
Email: djtantillo@ucdavis.edu

their occurrence specifically in proteins. On the basis of this data, we also provide recommendations for computational chemists modelling systems containing such interactions.

2. Computational approaches for modelling noncovalent interactions

2.1. Geometries

The initial step of a computational study on noncovalent interactions generally involves determining a reasonable geometry for the system of interest. Strengths of noncovalent

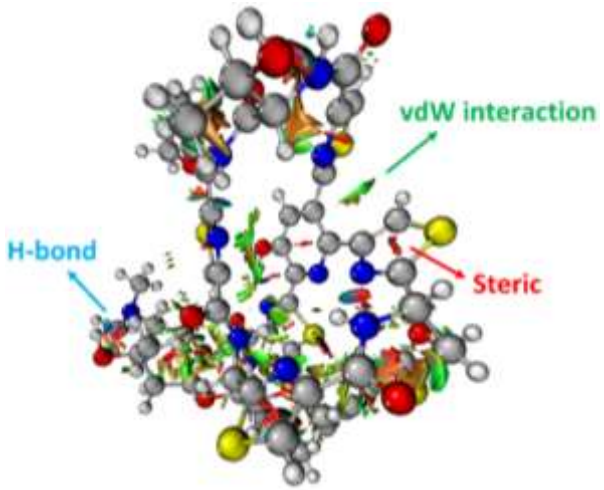

Fig. 1 The NCI plot of Glycothiohexide α.[46]

interactions, and contributions to these strengths from different physical factors, are geometry (distance, angle, etc.) dependent.[20,21] In general, one is interested in the lowest energy conformer on a multidimensional potential energy surface. While the lowest energy conformers often correspond to bioactive conformers, one should keep in mind that that need not always be the case. There are many conformational sampling algorithms that vary in accuracy and computational time.[22–29] A systematic search would explore the whole potential energy surface (PES) for each degree of freedom; that completeness comes at a high computational cost, however. In contrast, a knowledge-based approach would be faster, since it would cover only a portion of the conformational space, but if it covers the relevant portion then all is well. Random searches (e.g., Monte Carlo) and simulated annealing (artificially applying a high temperature to get over barriers) can be used to attempt to sample multiple regions of a PES. Molecular dynamics (MD) can be used to sample conformational changes over time. If one is interested in aqueous solution, then implicit or explicit solvent must be included as well. Detailed descriptions of these (and many other) techniques are beyond the scope of this review, but refs. 24-31 provide good starting points for interested readers. Sometimes the validity of a computed structure is assessed through comparison with experimental data (crystallography, NMR, circular dichroism, etc.).[29] However, the limits of these experimental methods should always be kept in mind, e.g., NMR shifts could represent contributions from several interconverting conformers, the geometric parameters obtained from an X-ray crystal structure may be influenced by crystal packing forces, etc.

2.2. Interaction energies

Prediction of protein-ligand binding affinity is an indispensable tool in drug discovery.[32-42] Here we are concerned, however, with the strengths of interactions between two protein substructures. Estimating such interaction energies is difficult. Often, what is done is to "cut" the groups of interest out of the protein context to arrive at a complex of two small molecules whose interaction energy can then be evaluated by comparing the energy of the complex with the energy of the two separate molecules. Such an estimate, of course, comes with caveats, the most significant being that the effects of the surrounding protein environment are not taken into account. That is okay, though, if one wishes to assess the *inherent* strength of an interaction.

2.3 Origins of attraction

The 3-dimensional structure of a protein is maintained through the interplay of multiple noncovalent interactions. Here we describe the commonly used theoretical approaches for assessing the origins of attraction (and repulsion) in noncovalent interactions. Note that these tools may provide numbers, but the results should be treated as qualitative in nature, given the issues described below.[32]

Noncovalent interaction (NCI) analysis[33] is a popular method for visualizing the noncovalent interaction regions in molecules. Users can generate color-coded reduced density gradient isosurfaces (NCI plots) in which blue, green and red represent strong attraction, weak (typically, van der Waals) attraction, and strong repulsion, respectively (Fig. 1). For large, complex systems, it is not convenient to use routine NCI analysis. One solution is to apply NCI analysis based on promolecular density in which predetermined electron density of the atoms in their free-states is used. Alternatively, independent gradient model (IGM) analysis based on promolecular density can also be applied to large systems at a reduced computational time and cost.[34] Also, with the IGM method, one can visualize interactions at a specific region of interest rather than visualizing all the interactions present within the system. Program packages such as *Multiwfn* support these types of wavefunction analysis.[35]

Another approach, the quantum theory of atoms in molecules (QTAIM),[36,37] is used to characterize the properties of chemical bonds via a topological analysis of electron density. In QTAIM, the presence of a bond critical point (BCP) is often used to argue for bonding between atoms. It has been argued that at a BCP, for some cases, the sign of the energy density may correspond to the nature of the bond, positive and negative values representing noncovalent and covalent interactions, respectively.[38] This argument has been extended to a point where a positive value of energy density per unit electron at a BCP (also defined as bond degree) represents a noncovalent

bond and hence, a weak interaction.[39] While the exact connections between the quantities computed with QTAIM and the bonding concepts used by organic and bioorganic chemists are still argued about, this tool can still prove useful for comparing interactions to each other.

Natural bond orbital (NBO)[40] calculations allow for the computation of orbital interaction energies between NBOs that correspond to localized (2-center 2-electron, Lewis-like) bonds. Second-order perturbation NBO energies provide estimates of contributions from donor-acceptor (filled-empty) and donor-donor (filled-filled) orbital interactions.

Another approach is energy decomposition analysis (EDA).[41] This widely used tool partitions interaction energies between two moieties into physically meaningful components such as exchange-repulsion, electrostatics, polarization and charge-transfer. Since there are many possible ways of partitioning energy, there exist different types of EDA approaches that can be classified into two main groups: variational and perturbation-based methods. Variational methods such as Kitaura-Morokuma analysis,[42,43] and absolutely localized molecular orbital EDA (ALMO EDA)[44] use intermediate wavefunctions (which provide expression for the monomers) to decompose interaction energy. On the other hand, in perturbation-based methods such as symmetry-adapted perturbation theory (SAPT),[45] the interaction energy is constructed as perturbative corrections to the isolated fragments. We direct our readers to Phipps et al.'s review for detailed descriptions and comments on limitations of the EDA methods used in biomolecular systems.[41]

For a representative recent example of the application of these techniques, see our recent study on the nature of noncovalent interactions involving sulfur atoms in the thiopeptide antibiotics glycothiohexide α and nocathiacin I.[46]

3. Noncovalent interactions involving sulfur atoms

We catalogue different types of sulfur noncovalent interactions present in biological systems below. Both experimental and computational studies that address energetic and geometric contributions of sulfur-based noncovalent interactions to stability and bioactivity are reviewed.

3.1. Hydrogen bonds involving sulfur atoms

Whereas the thioether-containing Met sidechain can accept hydrogen bonds, the thiol-containing Cys can both accept and donate hydrogen bonds.[47] Furthermore, the sulfur atoms in disulfide bonds can form bifurcated hydrogen bonds, i.e., hydrogen bonding motifs that include both sulfur atoms acting as hydrogen bond acceptors.[48,49] While the majority of hydrogen bond lengths observed in proteins range from 2.7 to 3.3 Å[50], sulfur containing hydrogen bonds are longer compared to hydrogen bonds where oxygen and nitrogen atoms are involved, since sulfur is a highly polarizable atom with a comparatively large atomic radius. In addition, electronegativity is key to the strength of hydrogen bonds, and sulfur is less electronegative (2.58 on the Pauling scale) than oxygen (3.44) and nitrogen (3.04), suggesting that its hydrogens bonds might be weaker. Nonetheless, these weak interactions can be important contributors to the overall shapes of proteins.[51,52]

3.1.1. S•••H-O type hydrogen bonds

The origin of the stability of *S•••H-O type* hydrogen bonds comes, at least in part, from the charge on the acidic hydrogen of the OH group interacting with sulfur.[49] Wennmohs et al. calculated the S•••H-O interaction energy (at the coupled cluster level) for the dimethylsulfide-methanol complex, in which dimethylsulfide acts as hydrogen bond acceptor and methanol acts as hydrogen bond donor, to be ~-5.5 kcal mol^{-1}. NBO analysis suggested that a major source of stabilization was the interaction of the sulfur 3p lone pair and the H-O σ* antibonding orbital.

While O•••H-O type hydrogen bonds are generally dominated by electrostatic effects, which are smaller for S•••H-O type hydrogen bonds, the contribution of dispersion interactions is larger in S•••H-O type hydrogen bonds due to the high polarizability of sulfur.[47,53] Biswal et al. used complexes between thioethers and *para*-cresol to mimic S•••H-O interactions between Met and tyrosine (Tyr). Their experimental and computational results show that O•••H-O hydrogen bonding is stronger than that of S•••H-O hydrogen bonding, but, for S•••H-O interactions, the longer the alkyl chain in the acceptor, stronger the binding of the complex,[47] hinting at effects beyond direct hydrogen bonding. A representative example of an S•••H-O type hydrogen bond in a protein, here a Met–Tyr interaction of the type examined by Biswal et al., is shown in Fig. 2.[54]

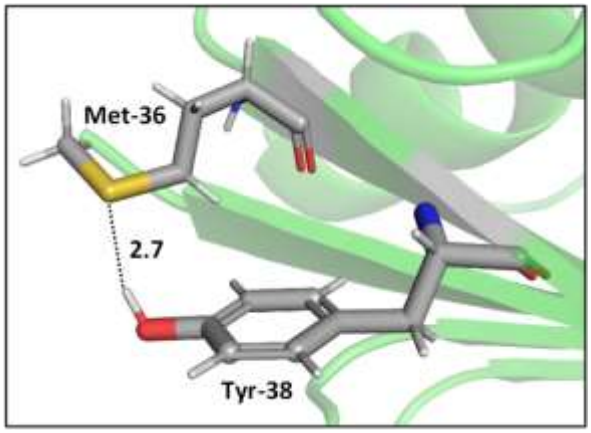

Fig. 2 S•••H-O hydrogen bonding interaction between the S of Met-36 and O-H of Tyr-38 (PDB ID: 1A2Z [54]). Distances shown in Å.

Gregoret et al. surveyed 85 protein structures for hydrogen bonds involving sulfur atoms. They found that hydrogen bonding is not common for Met residues, which could be attributed to the hydrophobic nature of Met. On the other hand, they observed that deprotonated Cys can act as an acceptor of hydrogen bonds from hydroxyl groups. Their study revealed that Cys residues participate in hydrogen bonding more abundantly. Thus, they suggest that Cys's propensity for participating in hydrogen bonding between the thiol group of a

Cys (*i*) and the carbonyl oxygen of residue *i-4* may have a direct influence helical conformational preferences.[48]

In addition, a statistical analysis conducted on >500 protein structures by Zhou et al. suggested that bifurcated hydrogen bonds involving sulfur contacts are prevalent in proteins. For instance, Fig. 3 shows a bifurcated hydrogen bond between two sulfur atoms of a disulfide bond (Cys-58 and Cys-63 residues) acting as acceptors and Thr-339 acting as donor. This interaction unites two α helices.[49,55]

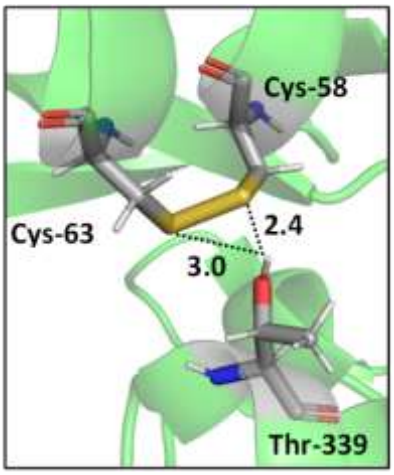

Fig. 3 A bifurcated hydrogen bond formed between the hydroxyl group in Thr-339 and the two sulfur atoms in disulfide bond Cys-58-Cys-63 (PDB ID: 3GRS). Distances shown in Å.[49,55]

However, based on the NCI analyses, the interactions in DMA-DME complex appeared to be more localized, which was taken as an indication of the larger dispersion interactions in the DMA-DMS complex.[56]

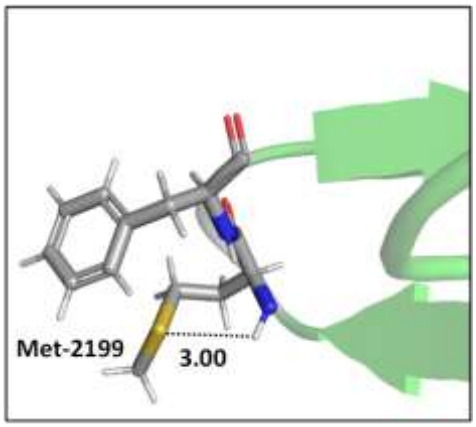

Fig. 4 The local folding of Met-2199 via S•••H-N hydrogen bonding interaction. (PDB ID: 1D7P [58]). Distances shown in Å.

Mons and co-workers reported a combined gas-phase spectroscopy and quantum chemistry study on S•••H-$N_{backbone}$ hydrogen bonds in *N*-acetyl-L-phenylalaninyl-L-methionine-amide and *N*-acetyl-L-methioninyl-L-phenylalanine-amide dipeptides in solvent-free environments by created using a supersonic expansion.[57] Both systems showed a local folding of the Met side-chains associated with hydrogen bonds between the sulfur and the neighboring NH(*i*) or NH(*i+1*) amides of the backbone. At 300 °K the stability brought by the Met side-chain folding was predicted to be ~2 kcal mol^{-1} (at the RI-B97-D/QZVPP level). An example of the local folding of Met residues via hydrogen bonding in the context of a protein is shown in Fig. 4.[58]

			geometry		interaction energy (ΔH, kcal/mol)	
entry	X	Y	*d* (Å)	θ (deg)	gas phase	water (SMD)
1	O	O	1.92	116	-7.27	-3.06
2	S	O	1.89	116	-8.86 (-1.58)[a]	-4.00 (-0.93)[a]
3	O	S	2.45	97	-6.89 (+0.38)[a]	-3.30 (-0.23)[a]

Table 1 Geometry dependence of hydrogen bonding interaction of thioamide and amide isosteres. [a] Numbers in parentheses are the relative energies with respect to entry 1. Interaction energies are calculated at CCSD(T)-SMD/aug-ccpVDZ//ωB97XD-SMD/aug-cc-pVDZ level of theory. Electrostatic potential maps generated at B3LYP/6-311+g(d,p) with an isovalue of 0.04. Adapted with permission from B. J. Lampkin and B. VanVeller, *J. Org. Chem.*, 2021, **86**, 18287–18291. Copyright 2021 American Chemical Society.

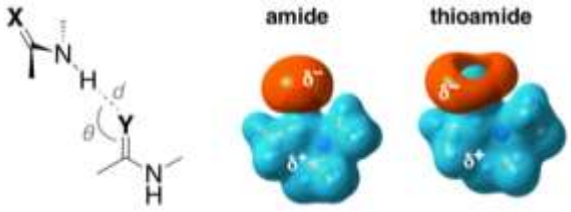

3.1.2. S•••H-N type hydrogen bonds

Kjaergaard and co-workers analyzed O•••H-N and S•••H-N interactions in dimethylamine-dimethyl ether (DMA-DME) and dimethylamine-dimethylsulfide (DMA-DMS) complexes and found that both complexes have similar binding energies.[56]

Lampkin and VanVeller, studied the influence of geometry and dielectric properties on the strength of S•••H-N hydrogen bonding in thioamides and showed that hydrogen bonds involving thioamides as hydrogen bond donors range in strength from 1.0-1.5 kcal mol^{-1}.[59] They reported that hydrogen

bonding contact angle (Table 1) is strongly affected by the nature of the hydrogen bond donor and acceptor. For instance, they calculated an optimized hydrogen bonding contact angle of 116° when the thioamide and amide are hydrogen bond donor and acceptor, respectively (Table 1, entry 2). However, an optimized hydrogen bonding contact angle of 97° was found when the hydrogen bond acceptor and donor are thioamide and amide, respectively (Table 1, entry 3), which is consistent with the involvement of a σ-hole in the thioamide electrostatic potential map (Table 1, top right). Overall, they showed that the thioamides act as good hydrogen bond acceptors when the hydrogen bond contact angle is between 90° and 100°, whereas amides can tolerate different angles.[59] The geometry of these hydrogen bonds appears to be determined mainly by dipole-dipole interactions.[60]

The energy associated with hydrogen bonds is sensitive to the environment. Hydrogen bonds in vacuum and hydrophobic environments are generally much stronger than hydrogen bonds in polar environments like water. This reduction in the strength can be attributed in part to screening of attractive electrostatic interaction and to entropic effects. Lampkin and VanVeller's study exemplifies the effect of solvent as well.[59] They tested the strength of S•••H-N hydrogen bonds in implicit water solvent and found weaker interactions than that in the gas phase. Moreover, they found that thioamides are slightly stronger hydrogen bond acceptors compared to amides in polar media. With regard to entropy, in vacuum, peptide side-chains fold back to form internal hydrogen bonds, whereas in water they have other options.[60–62]

3.1.3. S-H•••O type hydrogen bonds

The statistical analysis conducted by Zhou et al. mentioned above also suggests that it more likely for Cys to act as a hydrogen bond donor than a hydrogen bond acceptor (donor-acceptor ratio 5:1).[20] Paul and Thomas studied S-H•••O hydrogen bonds using local energy decomposition (LED)[63] analysis on different thiol-water complexes and showed that the binding energy of the resulting hydrogen bonds ranges from -2.1 to -3.6 kcal mol^{-1} and the dominant source of stabilization in these complexes was electrostatic attraction.[64] NBO analysis on these systems also pointed to the importance of $O_{lp} \leftrightarrow \sigma^*_{S-H}$ orbital interactions (the natural orbital interaction energies for selected thiol-water complexes varied from ~3-5.5 kcal mol^{-1} at the B3LYP/cc-pVTZ level of theory).

3.1.4. S-H•••N type hydrogen bonds

Mielke and co-workers studied O-H•••N and S-H•••N interactions in CH_3OH•••NH_3 and CH_3SH•••NH_3 complexes.[65] They reported a larger interaction energy for CH_3OH•••NH_3, inconsistent with the stronger aqueous acidity of CH_3SH compared to CH_3OH. Jaju et al. calculated the S-H•••N hydrogen bonding stabilization energy in the [4-H-C_5H_4-N•••H-SH] complex to be ~3 kcal mol-1, which is ~1 kcal mol^{-1} larger than the S-H•••O interaction in the SH_2•••CH_3OH complex (at the MP2/aug-cc-pVTZ level),[66] perhaps due simply to the higher basicity of the N atom than the O atom. The distances for the S-H•••N and S-H•••O hydrogen bonds in these complexes are predicted to be 2.08 Å and 2.10 Å, respectively. Although the major source of stability of the S-H•••N hydrogen bond is predicted to come from donor-acceptor interactions ($N_{lp} \leftrightarrow \sigma^*_{S-H}$), electrostatic and dispersion interactions are also important contributors.

3.2. S•••O and S•••N interactions

Although sometimes overlooked, S•••O and S•••N interactions are common in biological systems. For example, more than two decades ago, Nagao et al. revealed that an S•••O interaction (~2.5 Å) was present in the (acylimino)thiadiazoline moiety of a class of angiotensin II receptor antagonists.[67] In general, an interatomic S•••O distance shorter than the sum of sulfur and oxygen van der Waals radii (3.32 Å) is taken as an indication of the presence of a favorable S•••O interaction. While there is some debate over the origins of close S•••O and S•••N contacts,[68] both electrostatic and dispersion interactions are known to contribute and these can be comparable in strength.[69] The electrostatic stabilization comes from attraction between partially positively charged sulfur (note that sulfur is not very electronegative and is frequently found near to electron-withdrawing groups in biological settings) and partially negatively charged oxygen or nitrogen.[12] In addition to electrostatic and dispersion interactions, donor-acceptor orbital interactions (e.g., $O_{lp} \leftrightarrow \sigma^*_{S-X}$) also are significant for the directional preference of S•••O and S•••N contacts,[70] even if these are counterbalanced by S lone pair/O or N lone pair repulsion.[68] Recently, Biswal et al. found that second-order interaction energies associated with donor-acceptor orbital interactions ($O_{lp} \leftrightarrow \sigma^*_{S-C}$) are typically ~2 kcal mol^{-1} and ~1 kcal mol^{-1} for small molecules obtained from the Cambridge Structural Database (CSD) and the Protein Data Bank (PDB), respectively.[71]

3.3. Interactions involving π-systems

A statistical analysis on sulfur-aromatic interactions was carried out by Zauhar et al. by collecting all crystal structures that contain at least one divalent sulfur atom and a phenyl ring from the Cambridge Crystallographic Database.[72] The results suggest that, for an ideal interaction the sulfur-aromatic distance should be ~5 Å and the sulfur should be placed in the plane of the ring as opposed to the trend observed for proteins, which places sulfur above the ring plane. This contradiction may be attributed to the stacking interactions present in small planar molecules that favor edge-on interactions or to the crystal packing forces that play crucial roles in controlling overall geometries, especially when weak interactions are involved. Energy analysis showed that a single sulfur-aromatic interaction

contributes ~1-2 kcal mol^{-1} to the stability of a protein and involves both van der Waals and electrostatic components, with their relative contributions varying with structure. There are several common structural motifs in which sulfur atoms are ~5 Å away from aromatic rings, differing by which, if any, groups shield the sulfur atom from the π-electrons of the aromatic system.

3.3.1. SC-H•••π interactions

One important sulfur-based interaction that contributes to protein structure is the SC-H•••π interaction, which is mainly observed in the hydrophobic cores of proteins.[16,17,73] SC-H•••π interactions were first analyzed by Morgan et al. in the 1970s.[74] The analysis of eight small globular proteins revealed the presence of SC-H•••π contacts between sidechains. A follow up study by Reid et al. showed that, in contrast to OC-H and NC-H groups, SC-H groups tend to interact away from the center of the aromatic rings.[75] Compared to a hydrophobic interaction with sulfur traded for an alkyl group, SC-H•••π interactions are more stable at greater distances, which can be attributed to dispersion interactions involving the polarizable sulfur atom.[69,76] While SC-H•••π interactions are largely dispersive in nature, electrostatics do influence orientational preferences.[17,72,77]

Pranata investigated dimethyl sulfide (DMS)-benzene complexes, models of a Met sidechain and an aromatic residue, in detail.[78] Three different orientations of DMS-benzene complexes were studied (Fig. 5). Ab initio calculations based on isolated molecules (not necessarily PES minima) predicted that complex I (Fig. 5) had the largest interaction energy (-2.9 kcal mol^{-1} at the MP2/6-31G* level) and the shortest contact distance from the sulfur atom to the center of the benzene ring (4.9 Å) (compared to complex II and complex III). Note that upon full optimization of complex II at the MP2/6-31G* level, a structure similar to complex I, but with the DMS horizontally displaced, was generated, which also was predicted to have an interaction energy of -2.9 kcal mol^{-1}. This study also suggested that the molecular mechanics force fields AMBER95 and OPLS-AA can reproduce the MP2/6-31G* results.

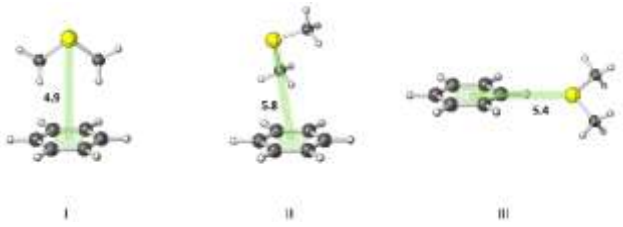

Fig. 5 Three different orientations of DMS-benzene complexes. I) The sulfur atom is placed on the symmetry axis of the benzene ring and the two methyl groups are directed towards the face of the benzene ring. II) One of the methyl groups oriented towards the face of the benzene ring. III) The sulfur atom is pointed towards the edge of the benzene ring. Distances shown in Å. [78]

Interactions analogous to those in complex II (Fig. 5) are found in proteins crystal structures. For example, Di Lello et al. determined the structure of a complex formed by the interaction between the amino-terminal transactivation domain of p53 and the pleckstrin homology domain of transcription factor b1 (Tfb1) by high-resolution NMR. In the Tfb1/p53 binding interface (shown in Fig. 6) the Met-59 residue participates in sulfur- π interactions with Trp-53. Additional contacts present between the isoleucine (Ile) and phenylalanine (Phe) residues of p53 and the Met residues of Tfb1 contribute to the overall stability of the complex. [79]

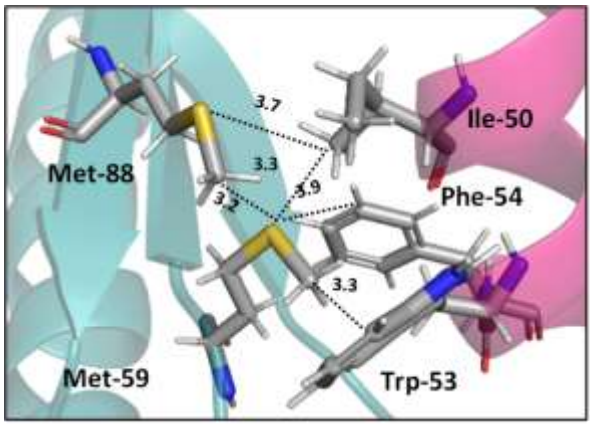

Fig. 6 Crystal structure of Tfb1 (green) / p53 (orange) complex (PDB ID: 2gs0) showing Tfb1-Met/p53-Ile, Tfb1-Met/p53-Phe and Tfb1-Met/p53-Trp interactions. Distances shown in Å. [79]

Fig. 7 π-type IND·H_2S complex. Distances shown in Å. [80]

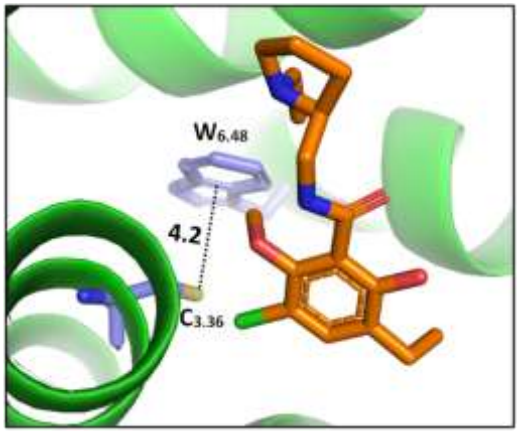

Fig. 8 The cocrystal structure (PDB ID: 3PBL) of the dopamine D_3 receptor bound to antagonist eticlopride (in orange). Distances shown in Å.[82]

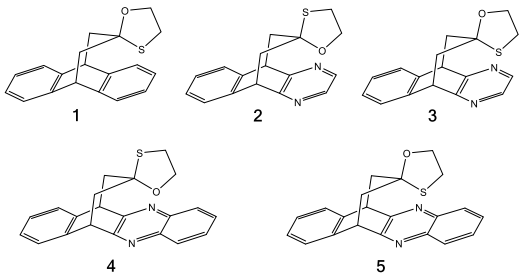

Fig. 9 π systems studied by Motherwell et al. to compare S•••π versus O•••π noncovalent interactions.[83]

3.3.2. S-H•••π interactions

Sherrill and co-workers studied the interaction of H_2S with benzene, which can be considered to be a small model of Cys interacting with an aromatic sidechain.[77] They found that the electrostatic interaction (-2.4 kcal mol^{-1}) arising from the partial positive charge on the H_2S hydrogens and the partial negative charge in the benzene π-cloud leads to substantial attraction, while the dispersion energy (-4.2 kcal mol^{-1}) provides an even larger attractive component.

The S-H•••π interactions in indole·H_2S (IND·H_2S) and 3-methylindole·H_2S (3-MI·H_2S) complexes were studied by Biswal and Wategaonkar, models of Cys interacting with the sidechain of tryptophan (Trp).[80] Both *σ*-type (O-H•••S and N-H•••S; see sections 3.1.1-2) and π-type (S-H•••π; Fig. 7) complexes were investigated. Computations at the MP2/aug-cc-pVDZ level of theory suggested that the binding energies for π-type and *σ*-type IND·H_2S complexes are -4.9 and -2.7 kcal mol^{-1}, respectively. Similarly, the binding energies for π-type and *σ*-type 3-MI·H_2S complexes are -5.2 and -2.7 kcal mol^{-1}, respectively. In contrast, for IND·H_2O and 3-MI·H_2O complexes, *σ*-type complexes are preferred. Moreover, they found that the S-H•••π interaction was stronger than other X-H•••π (X = C, N, O) interactions.

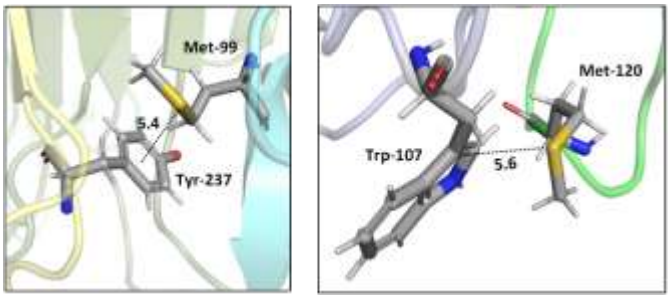

Fig. 10 Crystal structures of TRAIL-DR5 showing DR5-Met/TRAIL-Tyr interaction (left, PDB ID: 1d0g) and LTα-TNFR1 showing TNFR1-Trp/LTα-Met interaction (right, PDB ID: 1tnr). Both Met-aromatic contacts are at around 5 Å separation. Distances shown in Å. [76]

3.3.3. S•••π interactions

Dougherty and co-workers showed that direct S•••π interactions are functionally important in the maintenance of a tightly packed microdomain functioning as a unit in the dopamine D2 receptor.[81] They used the crystal structure of the dopamine D3 receptor[82] as a model (Fig. 8) and located a highly conserved microdomain. Mutant cycle analysis and unnatural amino acid mutagenesis on the residues in this microdomain in the related D2 receptor suggested that the strong interaction between Trp and Cys residues in which the sulfur containing side chain of a Cys residue points to the face of the aromatic ring of a Trp contributes to the rigidity of the microdomain.

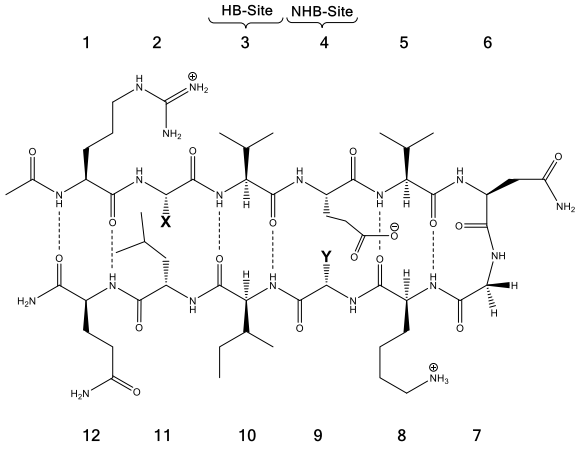

Fig. 11 The model system consisting of 12 amino acids. X (= Phe, Trp, Cha) and Y (= Lys, Nle, Met) are the diagonal interacting residues. The hydrogen bonded and nonhydrogen-bonded sites are abbreviated as HB-site and NHB-site, respectively.[86]

To compare the strengths of direct interactions between the π-faces of aromatic rings with oxygen and sulfur, Motherwell et al. prepared the series of oxathiolanes shown in Fig. 9 (and others), which can adopt conformations with either an oxygen or sulfur atom proximal to an aromatic ring.[83] Based on their results, it appears that (a) oxygen atoms do not like to be near the π-faces of electron-rich aromatics, (b) sulfur atoms do not mind being near the π-faces of electron-rich aromatics, (c) oxygen atoms do not mind being near the π-faces of electron-poor aromatics. While it is difficult to pin down the relative contributions of attraction and repulsion in such systems, it is clear that sulfur can reside near the π-face of aromatics, even electron-rich ones, likely a consequence of its polarizability.

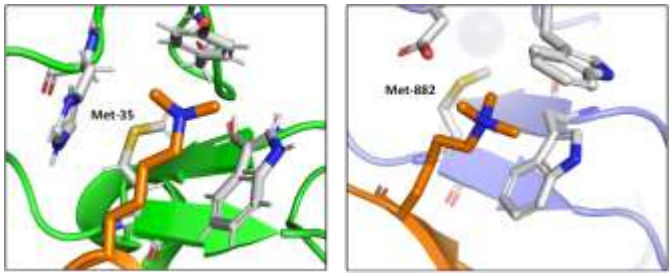

Fig. 12 The molecular recognition of H3K4me3 (in orange) by DIDO1 (in green, PDB ID: 4L7X) and TAF3 (in purple, PDB ID: 5WXH).[87]

Viguera and Serrano's work on sidechain interactions between sulfur containing amino acids (Cys and Met) and phenylalanine (Phe) residues — the first experimental analysis probing helix stability mediated by Phe and Cys/Met interactions — showed that these interactions are related directly to the stability of α helices.[84,85] The origins of this α helix stability appears to come from both the hydrophobic nature of

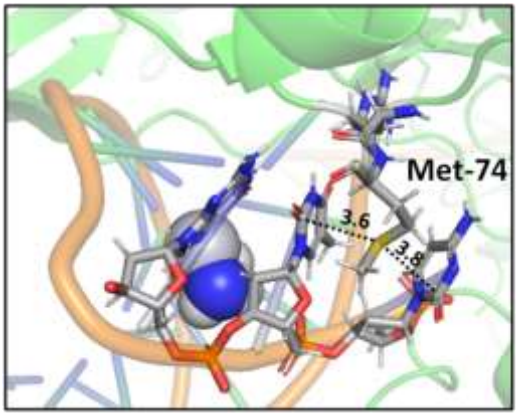

Fig. 13 Crystal structure of cisplatin–(1,3-GTG) lesion in complex with DNA Polymerase η (PDB ID: 2WTF). The Met residue surrounded by nucleobases blocks the movement of the polymerase along the DNA strand. Distances shown in Å. [88]

the aromatic rings and the electrostatic interactions between the S and the aromatic ring (primarily dispersion).

Two tumor necrosis factor (TNF) ligand-receptor complexes TRAIL-DR5 and LTα-TNFR1 were examined both experimentally via vitro cellular experiments and computationally to probe the role of the Met-aromatic binding motif.[76] DR5-Met/TRAIL-Tyr (left) and TNFR1-Trp/ LTα-Met (right) interactions are shown in Fig. 10. Molecular dynamics simulations were used to obtain

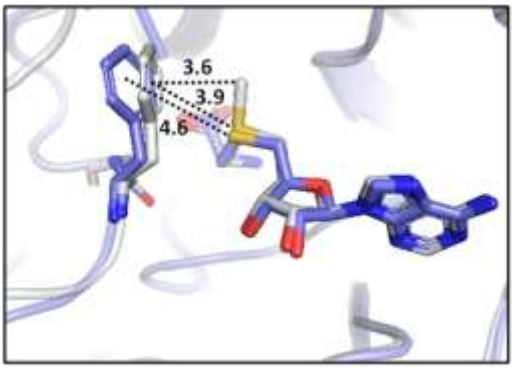

Fig. 14 Aromatic interactions of T. thermophilus ribosomal protein L11 methyltransferase with SAM (PDB ID: 2NXE, in gray) and SAH (PDB ID: 3EGV, in plum).[89]

bioactive conformers that match with those in the Protein Data Bank (PDB). The results from quantum mechanical calculations suggested that dispersive sulfur-aromatic interactions at around 5 Å separation provide extra stability (~1-1.5 kcal mol^{-1}) to the protein compared to interactions within their analogues where sulfur was replaced with CH_2. Note that SC–H•••π interactions (section 3.3.1) may also contribute here (and in the following cases).

Tatko and Waters investigated the nature of sulfur-π interactions in a β-hairpin by putting a Met residue diagonal to an aromatic ring (Trp or Phe) (Fig. 11).[86] The proximity between Met and the aromatic ring provides a suitable geometry for sulfur-π contacts to occur. They found that the Met significantly contributes to β-hairpin stability with a hydrophobic driving force (for instance, as determined by double-mutant cycles, Met-Phe interaction contributes -0.31 kcal mol^{-1}).

Albanese and Waters examined the role of sulfur in the Met residues in the binding of a gene expression regulator trimethyllysine (Kme3).[87] They probed the recognition of Kme3 by the Met containing aromatic cage in the reader proteins DIDO1 and TAF3 by systematic mutational studies (Fig. 12). For both systems, they observed a change in the NMR chemical shifts of the Met residue upon binding histone 3 K4me3 (H3K4me3), which indicated the presence of a binding interaction. Linear free energy relationships suggested that the origin of this Met-Kme3 binding was dispersive, which again could be attributed to the high polarizability of sulfur. They also found that the charge on Kme3 did not alter the interaction with the Met, which suggested that the electrostatic interactions (sulfur-cation) do not contribute significantly to binding.[87]

A study on a cisplatin–(1,3-GTG) cross-Link within DNA Polymerase η revealed that the Met residue in the DNA polymerase η participates in sulfur-arene interactions, which helps maintain the folded geometry of the protein complex and blocks the movement of the polymerase along the DNA strand (Fig. 13).[88] In this complex, both S•••π and SC-H•••π interactions are present.

Recently, Waters and coworkers compared the strength of the sulfonium•••π, S•••π and ammonium•••π interactions in a β-hairpin peptide model system via a combination of computational studies and analysis of structures in the PDB.[89] They found that due to sulfur's higher polarizability, sulfonium•••π interactions are stronger than ammonium•••π interactions. Further comparison of sulfonium•••π and S•••π interaction energies by the analysis of S-adenosylmethionine (SAM) and S-adenosylhomocysteine (SAH)-bound proteins in the PDB highlighted the importance of charge. They found similar aromatic interactions between SAM and SAH except for the methyl•••π interaction that is only present in SAM which highly influences the bioactivity of SAM-dependent methyltransferases (Fig. 14).[89] This interaction is an example of a SC–H•••π interaction (section 3.3.1) enhanced by charge.

3.3.4. S•••$\pi^*_{C=O}$ interactions

n → π^* interactions resulting from the overlap of lone pairs (n) and π^* antibonding orbitals along the Bürgi-Dunitz trajectory play an important role in maintaining the conformational stability of proteins (Fig. 15).[90,91] Similar to the observations of Bürgi and Dunitz for other lone pair donors (Fig. 15.B, θ angle), Chakrabarti and Pal found that the preferred S•••C—O angle for the $n_s \rightarrow \pi^*_{C=O}$ interaction is 109° (± 15°).[92]

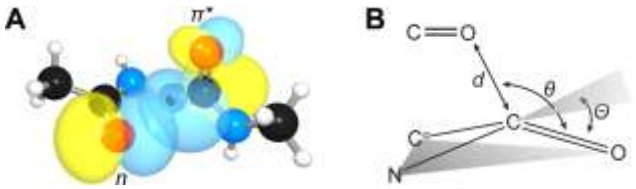

Fig. 15 A) n → π^* orbital interaction in the backbone of bitter gourd trypsin inhibitor (PDB: 1vbw), residues 5-7. (B) Geometric parameters characterizing n → π^* interaction (d: distance between the nucleophile and carbonyl; θ: Angle of the nucleophilic attack; Θ: degree of pyramidalization). Adapted with permission from R. W. Newberry, G. J. Bartlett, B. VanVeller, D. N. Woolfson and R. T. Raines, *Protein Sci.*, 2014, **23**, 284–288. Copyright 2014 John Wiley & Sons, Inc.

Many experimental and computational studies by Raines and co-workers have revealed the intricacies of stereo electronic effects in tuning the secondary structures of proteins, including the importance of n → π^* interactions.[11,93–100] For instance, Choudhary et al. explored the origin of carbonyl-carbonyl interaction in proteins and found that thioamides are better electron-pair donors compared to their amide counterparts.[93] Newberry et al. reported that the n → π^* interaction between amide carbonyl groups in proteins contributes ≥0.27 kcal mol^{-1}, and this magnitude triples when the interaction is between two thioamides due to better orbital overlap and a lower energy gap between donor and acceptor orbitals.[95] They also observed an increase in the pyramidalization of the acceptor C atom as the n → π^* interaction strengthens, consistent with work on related systems.[93,95,100–102] The stability of the collagen triple helix – which is highly affected by hydrogen bonds and n → π^* interactions[103] – was also shown to be increased upon replacement of backbone amides with thioamides.[94] Later, Kilgore at al. probed the importance of $n_S \rightarrow \pi^*_{C=O}$ interactions in Cys residues and disulfide bonds in proteins.[98] They found that $n_S \rightarrow \pi^*$ interactions provided enhanced stability and led to lowered pK_a values of N-terminal Cys residues of the CXXC motifs[104] (shown in Fig. 16), which are critical for redox functions. In addition, the strong $n_S \rightarrow \pi^*_{C=O}$ interactions present in vicinal disulfide bonds led to an electropositive (and hydrophobic site) for ligand binding.[98]

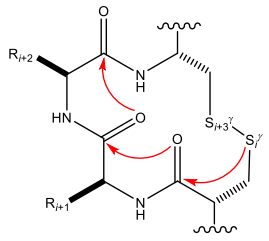

Fig. 16 The map of n → π^* interactions inside the CXXC motif.[98]

3.4. Generalizations

Table 2 represents the typical magnitudes and the major sources of stabilization for the sulfur noncovalent interactions reviewed here. However, we would like to warn our readers that the magnitude of stabilization may vary, since it highly depends on the system of interest and its environment.

Table 2 Current best estimates of typical magnitudes and the major sources of stabilization for the sulfur noncovalent interactions reviewed in this contribution.

Interaction Type	Typical Magnitude (kcal mol^{-1})	Major Sources of Stabilization
S-H•••O	~ 2-6	Electrostatics > Donor-Acceptor > Dispersion
S-H•••N	~ 3	Donor-Acceptor > Electrostatics > Dispersion
S•••H-O	~ 2-5	Dispersion > Electrostatics > Donor-Acceptor
S•••H-N	~ 2	Dispersion > Electrostatics > Donor-Acceptor
S•••O	~ 2-3	Dispersion ≈ Electrostatics > Donor-Acceptor
S•••N	~ 2-3	Dispersion ≈ Electrostatics > Donor-Acceptor
SC-H•••π	~ 3	Dispersion > Electrostatics > Donor-Acceptor
S-H•••π	~ 2-5	Dispersion > Electrostatics > Donor-Acceptor
S•••π	~ 0.3-3	Dispersion > Electrostatics ≈ Donor-Acceptor
S•••$\pi^*_{C=O}$	~ 0.25-3	Donor-Acceptor > Dispersion ≈ Electrostatics

4. Recommendations for modelers

Computational chemistry is an indispensable tool to study noncovalent interactions in biological systems. With the aid of quantum chemical calculations, one can investigate these interactions both qualitatively and quantitatively. Nowadays, most computational studies on noncovalent interactions are carried out using density functional theory (DFT),[105] a versatile computational modelling method for calculating the electronic structure of atoms and molecules. However, the choice of which method to use – DFT or a more expensive but more accurate method – depends on the system of interest. One generally faces a compromise between accuracy and computational cost (i.e., time for calculations to finish with available computer resources). Here, we recommend a few methods that have been found useful for studying noncovalent interactions involving sulfur atoms. The DFT functionals that account for dispersion correction such as ωB97X-D[106], M06-2X[107–109], PBE0-D3[110,111], B3LYP-D3(BJ)[105,112–114] have been commonly used in geometry optimizations and provided reasonable results.[53,56,64,71,115–118] Due to issues with DFT in describing the dispersion interactions, many have chosen second-order Møller–Plesset perturbation theory (i.e., MP2) or coupled cluster (CC) theory with single, double and perturbative triple excitations (i.e. CCSD(T)).[47,53,65,66,77,116,117,119–121,122] For small systems, these methods can be affordable. A study by Rothlisberger and co-workers showed that dispersion corrected atom centered potentials (DCACPs)[123,124] significantly improve the DFT description of the weak interactions of sulfur-containing molecules and the resulting DFT method correctly reproduces MP2 or CCSD(T) binding energies.[120] For basis sets, double-ζ or triple-ζ Pople type basis sets that include diffuse and polarization functions, Weigend's def2-TZVP[125,126] basis set, and Dunning's correlation-consistent cc-pVnZ or augmented correlation-consistent aug-cc-pVnZ (where n = D, T, or Q) basis sets[127–131] are commonly used in calculations on sulfur-based

noncovalent interactions.[53,56,119–121,64–66,71,77,115–117] To obtain reliable interaction energies, the counterpoise correction for basis set superposition error (BSSE)[132] and corrections for the harmonic zero-point vibrational energies are recommended, especially when small basis sets are used.[133–135]

If one wishes to include solvent in one's modelling, there are three general approaches: implicit solvation, explicit solvation, and a hybrid of the two. In implicit solvation, the solvent is treated as a continuum with a certain dielectric constant (and other properties). In explicit solvation, the solvent is treated as discrete molecules. Hybrid solvation modelling involves using a few explicit solvent molecules with an implicit solvent model on top. Using an implicit model is the most affordable approach, but a hybrid approach can be used as a balancing act between a realistic and a cost-efficient treatment of solvent, especially if noncovalent interactions between solute and solvent are important.[136–138]

If one wishes to include a whole protein in one's modelling, the Quantum Mechanics/Molecular Mechanics (QM/MM) approach is the way to go. This approach was introduced by Warshel and Levitt in the 1970s.[139,140] The QM/MM method is an efficient way of studying large systems in which a small region of the system — that where the key chemical processes take place — is treated quantum-mechanically, while the remainder of the system is treated classically, e.g., using molecular mechanics or a force field. Recently, Jorgensen and co-workers developed a new force field that improved the representation of sulfur charge anisotropy and directional noncovalent interactions via the addition of off-atom charged sites,[141] a welcome development for those modelling systems with sulfur-based noncovalent interactions. In the popular multilayer approach known as ONIOM, a large biomolecule is divided into "n" number of layers and each layer is treated with a different model chemistry (i.e, ab initio, semi-empirical and molecular mechanics) at a reduced cost.[142,143] We recommend a careful consideration in choosing suitable QM and MM methods, how one partitions a system into QM and MM regions, and how one treats the interactions between QM and MM regions. Along these lines, we direct readers to recent reviews for a deeper dive into QM/MM modelling.[144,145]

5. Conclusion and outlook

While sulfur may not receive the same attention as carbon, hydrogen, nitrogen, and oxygen, it plays many important roles in biology. Here we have summarized the variety of types of noncovalent interactions in which it participates, each illustrated with examples from protein structures and accompanied by accounts of theoretical studies on preferred geometries and interaction energies. We hope that bringing these examples together will inspire readers not only to consider noncovalent interactions involving sulfur when examining structures of biological molecules that have captured their interest, but also to make use of them in designing new molecules of biological relevance.

6. Author Contributions

Both authors wrote and edited the text.

7. Conflicts of interest

The authors have no conflicts of interest to report.

8. Acknowledgements

We gratefully acknowledge continued financial and computational support from the US National Science Foundation.

9. References

1 K. A. Dill, *Biochemistry*, 1990, **29**, 7133–7155.
2 C. N. Pace and P. CN, *Trends Biotechnol.*, 1990, **8**, 93–98.
3 C. N. Pace, *Trends Biochem. Sci.*, 1990, **15**, 14–17.
4 S. R. Trevino, S. Schaefer, J. M. Scholtz and C. N. Pace, *J. Mol. Biol.*, 2007, **373**, 211.
5 M. C. Deller, L. Kong and B. Rupp, *Acta Crystallogr. Sect. F, Struct. Biol. Commun.*, 2016, **72**, 72.
6 M. L. Waters, *Pept. Sci.*, 2004, **76**, 435–445.
7 S. Jena, J. Dutta, K. D. Tulsiyan, A. K. Sahu, S. S. Choudhury and H. S. Biswal, *Chem. Soc. Rev.*, 2022, **51**, 4261–4286.
8 S. L. Cockroft and C. A. Hunter, *Chem. Soc. Rev.*, 2007, **36**, 172.
9 J. P. Wagner and P. R. Schreiner, *Angew. Chemie - Int. Ed.*, 2015, **54**, 12274–12296.
10 E. Persch, O. Dumele and F. Diederich, *Angew. Chem. Int. Ed. Engl.*, 2015, **54**, 3290–3327.
11 R. W. Newberry and R. T. Raines, *ACS Chem. Biol.*, 2019, **14**, 1677–1686.
12 F. T. Burling and B. M. Goldstein, *J. Am. Chem. Soc.*, 1992, **114**, 2313–2320.
13 J. C. Gómez-Tamayo, A. Cordomí, M. Olivella, E. Mayol, D. Fourmy and L. Pardo, *Protein Sci.*, 2016, **25**, 1517–1524.
14 W. Brandt, A. Golbraikh, M. Täger and U. Lendeckel, *Eur. J. Biochem.*, 1999, **261**, 89–97.
15 S. Hati and S. Bhattacharyya, *ACS Omega*, 2020, **5**, 16292–16298.
16 E. A. Meyer, R. K. Castellano and F. Diederich, *Angew. Chemie Int. Ed.*, 2003, **42**, 1210–1250.
17 L. M. Salonen, M. Ellermann and F. Diederich, *Angew. Chemie Int. Ed.*, 2011, **50**, 4808–4842.
18 B. R. Beno, K. S. Yeung, M. D. Bartberger, L. D. Pennington and N. A. Meanwell, *J. Med. Chem.*, 2015, **58**, 4383–4438.
19 C. Bissantz, B. Kuhn and M. Stahl, *J. Med. Chem.*, 2010, **53**, 5061–5084.
20 A. K. Vitek, T. M. E. Jugovic and P. M. Zimmerman, *ACS Catal.*, 2020, **10**, 7136–7145.
21 A. V. Brethomé, S. P. Fletcher and R. S. Paton, *ACS Catal.*, 2019, **9**, 2313–2323.
22 G. Olanders, H. Alogheli, P. Brandt and A. Karlén, *J. Comput. Aided. Mol. Des.*, 2020, **34**, 231–252.
23 T. Lewis-Atwell, P. A. Townsend and M. N. Grayson,

Tetrahedron, 2021, **79**, 131865.
24 J. C. Cole, O. Korb, P. McCabe, M. G. Read and R. Taylor, *J. Chem. Inf. Model.*, 2018, **58**, 615–629.
25 G. Klebe, *Perspect. Drug Discov. Des. 1995 31*, 1995, **3**, 85–105.
26 G. Sliwoski, S. Kothiwale, J. Meiler and E. W. Lowe, *Pharmacol. Rev.*, 2014, **66**, 334.
27 C. Liao, M. Sitzmann, A. Pugliese and M. C. Nicklaus, *Future Med. Chem.*, 2011, **3**, 1057.
28 A. Liwo, C. Czaplewski, S. Ołdziej and H. A. Scheraga, *Curr. Opin. Struct. Biol.*, 2008, **18**, 134.
29 N. Foloppe and I.-J. Chen, *Curr. Med. Chem.*, 2009, **16**, 3381–3413.
30 K. N. Houk, A. G. Leach, S. P. Kim and X. Zhang, *Angew. Chemie Int. Ed.*, 2003, **42**, 4872–4897.
31 D. H. Williams, E. Stephens, D. P. O'Brien and M. Zhou, *Angew. Chemie Int. Ed.*, 2004, **43**, 6596–6616.
32 S. Scheiner, *J. Comput. Chem.*, 2022, **43**, 1814–1824.
33 E. R. Johnson, S. Keinan, P. Mori-Sánchez, J. Contreras-García, A. J. Cohen and W. Yang, *J. Am. Chem. Soc.*, 2010, **132**, 6498–6506.
34 C. Lefebvre, H. Khartabil, J. C. Boisson, J. Contreras-García, J. P. Piquemal and E. Hénon, *ChemPhysChem*, 2018, **19**, 724–735.
35 T. Lu and F. Chen, *J. Comput. Chem.*, 2012, **33**, 580–592.
36 R. F. W. Bader, *Chem. Rev.*, 1991, **91**, 893–928.
37 R. F. W. Bader, *Acc. Chem. Res.*, 1985, **18**, 9–15.
38 D. Cremer and E. Kraka, *Angew. Chemie Int. Ed. English*, 1984, **23**, 627–628.
39 E. Espinosa, I. Alkorta, J. Elguero and E. Molins, *J. Chem. Phys.*, 2002, **117**, 5529.
40 F. Weinhold, C. R. Landis and E. D. Glendening, *Int. Rev. Phys. Chem.*, 2016, **35**, 399–440.
41 M. J. S. Phipps, T. Fox, C. S. Tautermann and C. K. Skylaris, *Chem. Soc. Rev.*, 2015, **44**, 3177–3211.
42 K. Kitaura and K. Morokuma, *Int. J. Quantum Chem.*, 1976, **10**, 325–340.
43 K. Morokuma, *Acc. Chem. Res.*, 1977, **10**, 294–300.
44 R. Z. Khaliullin, E. A. Cobar, R. C. Lochan, A. T. Bell and M. Head-Gordon, *J. Phys. Chem. A*, 2007, **111**, 8753–8765.
45 B. Jeziorski, R. Moszynski and K. Szalewicz, *Chem. Rev.*, 1994, **94**, 1887–1930.
46 V. Kojasoy and D. J. Tantillo, *unpublished work*.
47 H. S. Biswal, *Challenges Adv. Comput. Chem. Phys.*, 2015, **19**, 15–45.
48 L. M. Gregoret, S. D. Rader, R. J. Fletterick and F. E. Cohen, *Proteins Struct. Funct. Bioinforma.*, 1991, **9**, 99–107.
49 P. Zhou, F. Tian, F. Lv and Z. Shang, *Proteins Struct. Funct. Bioinforma.*, 2009, **76**, 151–163.
50 D. F. Sticke, L. G. Presta, K. A. Dill and G. D. Rose, *J. Mol. Biol.*, 1992, **226**, 1143–1159.
51 I. G. Kamphuis, J. Drenth and E. N. Baker, *J. Mol. Biol.*, 1985, **182**, 317–329.
52 J. F. Bazan and R. J. Fletterick, *Proc. Natl. Acad. Sci. U. S. A.*, 1988, **85**, 7872.
53 F. Wennmohs, V. Staemmler and M. Schindler, *J. Chem. Phys.*, 2003, **119**, 3208–3218.
54 M. Singleton, M. Isupov and J. Littlechild, *Structure*, 1999, **7**, 237–244.
55 P. A. Karplus and G. E. Schulz, *J. Mol. Bid*, 1987, **195**, 701–729.
56 C. L. Andersen, C. S. Jensen, K. Mackeprang, L. Du, S. Jørgensen and H. G. Kjaergaard, *J. Phys. Chem. A*, 2014, **118**, 11074–11082.
57 H. S. Biswal, E. Gloaguen, Y. Loquais, B. Tardivel and M. Mons, *J. Phys. Chem. Lett.*, 2012, **3**, 755–759.
58 K. P. Pratt, B. W. Shen, K. Takeshima, E. W. Davie, K. Fujikawat and B. L. Stoddard, *Nature*, 1999, **402**, 439–442.
59 B. J. Lampkin and B. VanVeller, *J. Org. Chem.*, 2021, **86**, 18287–18291.
60 E. S. Feldblum and I. T. Arkin, *Proc. Natl. Acad. Sci. U. S. A.*, 2014, **111**, 4085–4090.
61 S. Y. Sheu, D. Y. Yang, H. L. Selzle and E. W. Schlag, *Proc. Natl. Acad. Sci. U. S. A.*, 2003, **100**, 12683–12687.
62 J. Gao, D. A. Bosco, E. T. Powers and J. W. Kelly, *Nat. Struct. Mol. Biol.*, 2009, **16**, 684–690.
63 W. B. Schneider, G. Bistoni, M. Sparta, M. Saitow, C. Riplinger, A. A. Auer and F. Neese, *J. Chem. Theory Comput.*, 2016, **12**, 4778–4792.
64 A. Paul and R. Thomas, *J. Mol. Liq.*, 2021, 118078.
65 K. Grzechnik, K. Rutkowski and Z. Mielke, *J. Mol. Struct.*, 2012, **1009**, 96–102.
66 K. Jaju, D. Pal, A. Chakraborty and S. Chakraborty, *Chem. Phys. Lett. X*, 2019, **4**, 100031.
67 Y. Nagao, T. Hirata, S. Goto, S. Sano, A. Kakehi, K. Iizuka and M. Shiro, *J. Am. Chem. Soc.*, 1998, **120**, 3104–3110.
68 B. M. Hudson, E. Nguyen and D. J. Tantillo, *Org. Biomol. Chem.*, 2016, **14**, 3975–3980.
69 F. Zhou, R. Liu, P. Li and H. Zhang, *New J. Chem.*, 2015, **39**, 1611–1618.
70 Y. N. Xiao and C. X. Zhang, *Bull. Chem. Soc. Jpn.*, 2002, **75**, 1611–1625.
71 H. S. Biswal, A. K. Sahu, B. Galmés, A. Frontera and D. Chopra, *ChemBioChem*, 2022, **23**, e202100498.
72 R. J. Zauhar, C. L. Colbert, R. S. Morgan and W. J. Welsh, *Biopolymers*, 2000, **53**, 233–248.
73 A. L. Ringer, A. Senenko and C. D. Sherrill, *Protein Sci.*, 2007, **16**, 2216.
74 R. S. Morgan, C. E. Tatsch, R. H. Gushard and P. K. Warme, *Int. J. Pept. Protein Res.*, 1978, **11**, 209–217.
75 C. Reid, P. F. Lindley and J. M. Thornton, *FEBS Lett.*, 1985, **190**, 209–213.
76 C. C. Valley, A. Cembran, J. D. Perlmutter, A. K. Lewis, N. P. Labello, J. Gao and J. N. Sachs, *J. Biol. Chem.*, 2012, **287**, 34979–34991.
77 T. P. Tauer, M. E. Derrick and C. D. Sherrill, *J. Phys. Chem. A*, 2005, **109**, 191–196.
78 J. Pranata, *Bioorg. Chem.*, 1997, **25**, 213–219.
79 P. Di Lello, L. M. M. Jenkins, T. N. Jones, B. D. Nguyen, T. Hara, H. Yamaguchi, J. D. Dikeakos, E. Appella, P. Legault and J. G. Omichinski, *Mol. Cell*, 2006, **22**, 731–740.
80 H. S. Biswal and S. Wategaonkar, *J. Phys. Chem. A*, 2009, **113**, 12774–12782.
81 K. N. M. Daeffler, H. A. Lester and D. A. Dougherty, *J. Am.*

Chem. Soc., 2012, **134**, 14890–14896.

82 E. Y. T. Chien, W. Liu, Q. Zhao, V. Katritch, G. W. Han, M. A. Hanson, L. Shi, A. H. Newman, J. A. Javitch, V. Cherezov and R. C. Stevens, *Science*, 2010, **330**, 1091–1095.

83 W. B. Motherwell, R. B. Moreno, I. Pavlakos, J. R. T. Arendorf, T. Arif, G. J. Tizzard, S. J. Coles and A. E. Aliev, *Angew. Chemie*, 2018, **130**, 1207–1212.

84 G. Némethy and H. A. Scheraga, *Biochem. Biophys. Res. Commun.*, 1981, **98**, 482–487.

85 A. R. Viguera and L. Serrano, *Biochemistry*, 1995, **34**, 8771–8779.

86 C. D. Tatko and M. L. Waters, *Protein Sci.*, 2004, **13**, 2515–2522.

87 K. I. Albanese and M. L. Waters, *Chem. Sci.*, 2021, **12**, 8900–8908.

88 T. Reißner, S. Schneider, S. Schorr and T. Carell, *Angew. Chemie - Int. Ed.*, 2010, **49**, 3077–3080.

89 K. I. Albanese, A. Leaver-Fay, J. W. Treacy, R. Park, K. N. Houk, B. Kuhlman and M. L. Waters, *J. Am. Chem. Soc.*, 2022, **144**, 2535–2545.

90 H. B. Biirgi, J. D. Dunitz and E. Shefter, *J. Am. Chem. Soc.*, 1973, **95**, 5065–5067.

91 C. Fufezan, *Proteins Struct. Funct. Bioinforma.*, 2010, **78**, 2831–2838.

92 P. Chakrabarti and D. Pal, *Protein Sci.*, 1997, **6**, 851–859.

93 A. Choudhary, D. Gandla, G. R. Krow and R. T. Raines, *J. Am. Chem. Soc.*, 2009, **131**, 7244–7246.

94 R. W. Newberry, B. VanVeller and R. T. Raines, *Chem. Commun.*, 2015, **51**, 9624–9627.

95 R. W. Newberry, B. Vanveller, I. A. Guzei and R. T. Raines, *J. Am. Chem. Soc.*, 2013, **135**, 7843.

96 R. W. Newberry and R. T. Raines, *Acc. Chem. Res.*, 2017, **50**, 1838–1846.

97 G. J. Bartlett, R. W. Newberry, B. Vanveller, R. T. Raines and D. N. Woolfson, *J. Am. Chem. Soc.*, 2013, **135**, 18682–18688.

98 H. R. Kilgore and R. T. Raines, *J. Am. Chem. Soc.*, 2018, **140**, 17606–17611.

99 G. J. Bartlett, A. Choudhary, R. T. Raines and D. N. Woolfson, *Nat. Chem. Biol.*, 2010, **6**, 615–620.

100 R. W. Newberry, G. J. Bartlett, B. VanVeller, D. N. Woolfson and R. T. Raines, *Protein Sci.*, 2014, **23**, 284–288.

101 G. A. Jeffrey, J. Mitra, K. N. Houk, N. G. Rondan and M. N. Paddon-Row, *J. Am. Chem. Soc.*, 1985, **107**, 321–326.

102 L. Esposito, L. Vitagliano, A. Zagari and L. Mazzarella, *Protein Sci.*, 2000, **9**, 2038.

103 M. D. Shoulders and R. T. Raines, *Annu. Rev. Biochem.*, 2009, 78, 929–958.

104 D. E. Fomenko and V. N. Gladyshev, *Biochemistry*, 2003, **42**, 11214–11225.

105 A. D. Becke, *J. Chem. Phys.*, 1998, **98**, 5648.

106 J. Da Chai and M. Head-Gordon, *Phys. Chem. Chem. Phys.*, 2008, **10**, 6615–6620.

107 Y. Zhao, D. G. Truhlar, Y. Zhao and · D G Truhlar, *Theor. Chem. Accounts 2007 1201*, 2007, **120**, 215–241.

108 Y. Zhao and D. G. Truhlar, *Acc. Chem. Res.*, 2008, **41**, 157–167.

109 N. Mardirossian and M. Head-Gordon, *J. Chem. Theory Comput.*, 2016, **12**, 4303–4325.

110 A. V. Vorontsov and P. G. Smirniotis, *J. Mol. Model.*, 2017, **23**, 223.

111 C. Adamo and V. Barone, *J. Chem. Phys.*, 1999, **110**, 6158.

112 S. Grimme, S. Ehrlich and L. Goerigk, *J. Comput. Chem.*, 2011, **32**, 1456–1465.

113 S. Tsuzuki and T. Uchimaru, *Phys. Chem. Chem. Phys.*, 2020, **22**, 22508–22519.

114 S. Grimme, J. Antony, S. Ehrlich and H. Krieg, *J. Chem. Phys.*, 2010, **132**, 154104.

115 S. Nikoo, Ph.D. thesis, University of Windsor, 2019.

116 H. S. Biswal, S. Bhattacharyya, A. Bhattacherjee and S. Wategaonkar, *Int. Rev. Phys. Chem.*, 2015, **34**, 99–160.

117 C. A. Morgado, J. P. McNamara, I. H. Hillier, N. A. Burton and M. A. Vincent, *J. Chem. Theory Comput.*, 2007, **3**, 1656–1664.

118 J. Sharma and P. A. Champagne, *J. Comput. Chem.*, 2022, 1.

119 B. J. Mintz and J. M. Parks, *J. Phys. Chem. A*, 2012, **116**, 46.

120 P. C. Aeberhard, J. S. Arey, I.-C. C. Lin and U. Rothlisberger, *J. Chem. Theory Comput.*, 2009, **5**, 23–28.

121 K. E. Riley and P. Hobza, *Wiley Interdiscip. Rev. Comput. Mol. Sci.*, 2011, **1**, 3–17.

122 K. Raghavachari, G. W. Trucks, J. A. Pople and M. Head-Gordon, *Chem. Phys. Lett.*, 1989, **157**, 479–483.

123 O. A. Von Lilienfeld, I. Tavernelli, U. Rothlisberger and D. Sebastiani, *Phys. Rev. Lett.*, 2004, **93**, 153004.

124 I. C. Lin, M. D. Coutinho-Neto, C. Felsenheimer, O. A. Von Lilienfeld, I. Tavernelli and U. Rothlisberger, *Phys. Rev. B - Condens. Matter Mater. Phys.*, 2007, **75**, 205131.

125 F. Weigend and R. Ahlrichs, *Phys. Chem. Chem. Phys.*, 2005, **7**, 3297–3305.

126 F. Weigend, *Phys. Chem. Chem. Phys.*, 2006, **8**, 1057–1065.

127 T. H. Dunning, *J. Chem. Phys.*, 1998, **90**, 1007.

128 R. A. Kendall, T. H. Dunning and R. J. Harrison, *J. Chem. Phys.*, 1998, **96**, 6796.

129 J. Dunning, K. A. Peterson and A. K. Wilson, *J. Chem. Phys.*, 2001, **114**, 9244–9253.

130 A. K. Wilson and T. H. Dunning, *J. Phys. Chem. A*, 2004, **108**, 3129–3133.

131 R. D. Bell and A. K. Wilson, *Chem. Phys. Lett.*, 2004, **394**, 105–109.

132 S. F. Boys and F. Bernardi, *Mol. Phys.*, 1970, **19**, 553–566.

133 A. L. Garden, J. R. Lane and H. G. Kjaergaard, *J. Chem. Phys.*, 2006, **125**, 144317.

134 J. A. Plumley and J. J. Dannenberg, *J. Comput. Chem.*, 2011, **32**, 1519–1527.

135 G. Pohl, J. A. Plumley and J. J. Dannenberg, *J. Chem. Phys.*, 2013, **138**, 245102.

136 W. Wu and J. Kieffer, *J. Chem. Theory Comput.*, 2019, **15**, 371–381.

137 J. Zhang, H. Zhang, T. Wu, Q. Wang and D. Van Der Spoel, *J. Chem. Theory Comput.*, 2017, **13**, 1034–1043.

138 R. Sure, M. el Mahdali, A. Plajer and P. Deglmann, *J. Comput. Aided. Mol. Des.*, 2021, **35**, 473–492.

139 A. Warshel and M. Levitt, *J. Mol. Biol.*, 1976, **103**, 227–249.

140 R. Estrada-Tejedor, L. Ros-Blanco and J. T. Closa, *Afinidad*,

2014, **71**, 89–94.

141 X. C. Yan, M. J. Robertson, J. Tirado-Rives and W. L. Jorgensen, *J. Phys. Chem. B*, 2017, **121**, 6626–6636.

142 M. Svensson, S. Humbel, R. D. J. Froese, T. Matsubara, S. Sieber and K. Morokuma, *J. Phys. Chem.*, 1996, **100**, 19357–19363.

143 L. W. Chung, W. M. C. Sameera, R. Ramozzi, A. J. Page, M. Hatanaka, G. P. Petrova, T. V. Harris, X. Li, Z. Ke, F. Liu, H. B. Li, L. Ding and K. Morokuma, *Chem. Rev.*, 2015, **115**, 5678–5796.

144 S. Ahmadi, L. Barrios Herrera, M. Chehelamirani, J. Hostaš, S. Jalife and D. R. Salahub, *Int. J. Quantum Chem.*, 2018, **118**, e25558.

145 R. P. Magalhães, H. S. Fernandes and S. F. Sousa, *Isr. J. Chem.*, 2020, **60**, 655–666.